3.4.3

Cyclotron-based high power neutron sources at PSI - operating experience and future outlook

D. Reggiani, D. Kiselev, T. Reiss, M. Seidel, R. Sobbia, V. Talanov and M. Wohlmuther

Paul Scherrer Institut, CH-5232 Villigen-PSI, Switzerland

E-mail: davide.reggiani@psi.ch

Abstract. The 1.4 MW PSI High Intensity Proton Accelerator (HIPA) operates concurrently two spallation sources, the continuous beam SINQ and the macro pulsed Ultra Cold Neutron (UCN) source. The paper discusses aspects related to beam operation, diagnostics and losses. Moreover, an outlook on the SINQ proton beam line upgrade projects currently under study like a beam flattening system as well as the design of a muon extraction channel are presented.

1. Introduction

The PSI high intensity proton accelerator (HIPA) generates a continuous wave (50.6 MHz frequency) 590 MeV, 1.4 MW beam [1]. A schematic of the accelerator complex is shown in Fig. 1. Protons are first brought to 870 keV by a Cockcroft-Walton generator and then transferred through a LEBT-section to the 72 MeV injector cyclotron. The medium energy beam is transferred to the 590 MeV ring cyclotron. High beam intensity can be achieved by limiting the extraction losses within the low 10^{-4} range, therefore preventing unsustainable machine activation. The 1.4 MW beam is first transported to a 5 mm thick meson production graphite target (M) where about 1% of the beam is lost. A second 40 mm thick graphite target (E) is mounted some 18 m downstream. About 8% of the beam is lost on the target itself while an additional 21% of it is absorbed by a collimator system that reshapes the highly divergent beam and protects accelerator components from activation and unnecessary beam load. The remaining beam is eventually transported to the SINQ neutron spallation source where it is completely stopped and absorbed. In case of a SINQ technical stop, the HIPA facility can still run at about 1 MW beam power (75% of the nominal intensity) due to a beam dump installed downstream of target E. A total of seven muon or pion secondary beam lines are located at the meson production targets M and E while SINQ provides neutrons for seventeen beam lines. In 2011 the ultra cold neutron (UCN) source was brought into routine operation at HIPA [2, 3]. This second spallation source runs concurrently to SINQ and is driven by macro pulses of the full 1.4 MW proton beam kicked into the UCN beam line with a typical duty cycle of about 1%. The switchover of a megawatt class beam between two beam lines is a unique feature of the PSI high intensity proton accelerator facility.

During the forty years of operation, the beam current of the PSI proton accelerator has been constantly increased from 0.1 to 2.4 mA. The aim for the next years is a further stepwise intensity upgrade that should bring the machine towards the 3.0 mA (1.8 MW) limit. However, some modifications in the transport of the high power beam are a prerequisite for reaching this

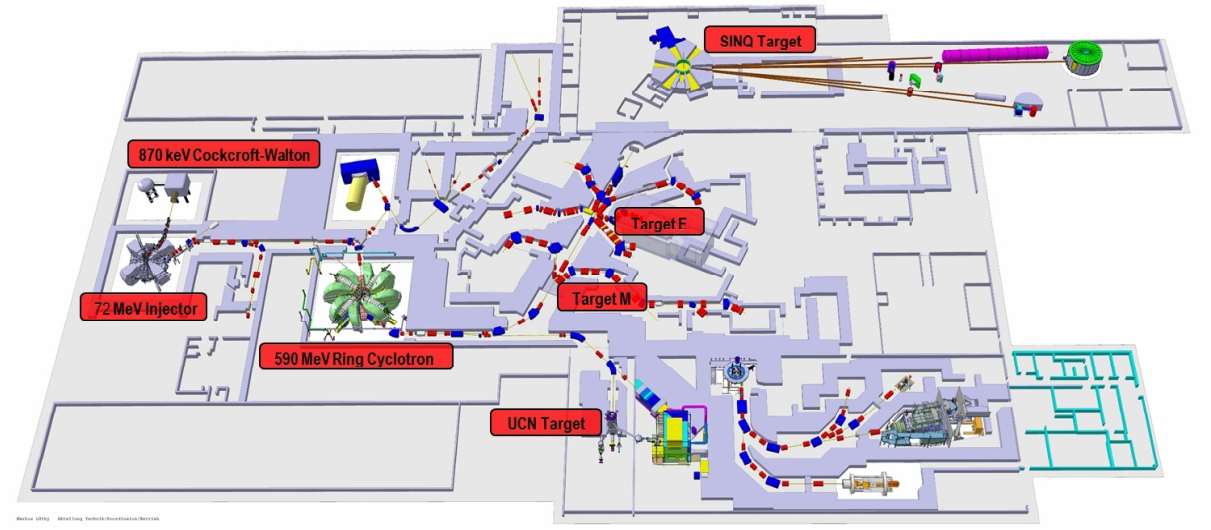

Figure 1. Overview of the PSI high intensity accelerator facility.

goal. One critical issue is the reduction of the beam losses downstream of target E, in particular on the collimator C2. Moreover, an additional increase of the beam current should be combined with a beam flattening system that would create a more uniform temperature distribution in the SINQ target. Another idea that was proposed recently is the possibility of extracting surface muons backscattered off the SINQ target and to guide them into a dedicated beam line. A two-year feasibility study is currently ongoing which should answer the question of the technical practicability.

2. Beam extraction

Extraction losses are usually the limiting factor of a high power cyclotron. At PSI, at the nominal beam intensity of 2.2 mA, the extraction losses are typically kept below 500 nA, which corresponds to the remarkable efficiency of 99.98%. Extraction losses result from the scattering of halo particles in the electrostatic deflector placed between the orbits of the last two turns. This effect can be minimized by providing a large orbit separation as well as by limiting the size of the beam deflector. Both these methods are applied at the PSI ring cyclotron. In an isochronous cyclotron the orbit separation is due to two different effects. The most obvious one is the acceleration term that causes a radius increment per turn given by:

$$\frac{dR}{dn_t} = \frac{R}{\gamma(\gamma^2-1)}\frac{U_t}{m_0c^2}$$

where U_t is the energy gain per turn, R the orbit radius and γ the relativistic factor. A large turn separation can therefore be obtained by building a large radius machine and by furnishing it with a powerful RF-system. In this way a large U_t or, respectively, a small number of turns N_t can be achieved. On the other hand, the relativistic term $\gamma(\gamma^2-1)$ disfavors the radius increment as the energy increases, thus limiting the maximum energy of a cyclotron accelerator to roughly 1 GeV. The extraction parameters of the PSI ring cyclotron are $R = 4460$ mm, $U_t \approx 3$ MeV, $\gamma = 1.63$. Plugged into the above equation, these figures give a radius increment between the last two turns of about 6 mm. This value can be substantially increased by exploiting the betatron motion of the beam around the ideal orbit. In fact, by carefully choosing the injection parameters, the phase of the horizontal betatron oscillation can be tuned in a way that at the location of the extraction deflector three turns overlap while the very last one gets a maximum

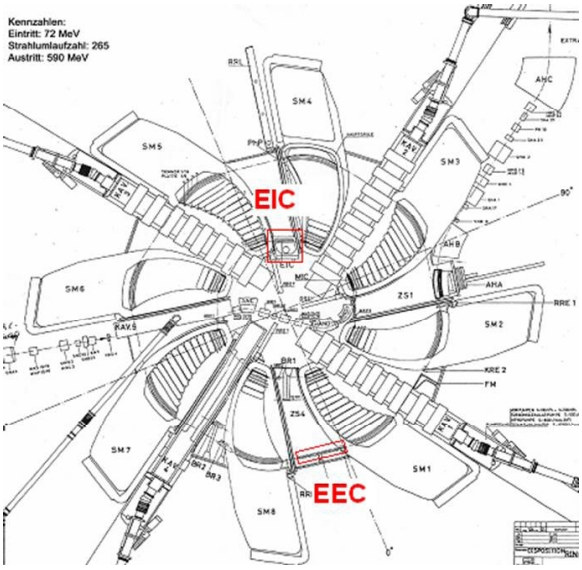

Figure 2. Drawing of the PSI 590 MeV ring cyclotron. The injection (EIC) and extraction (EEC) electrostatic elements are highlighted in red.

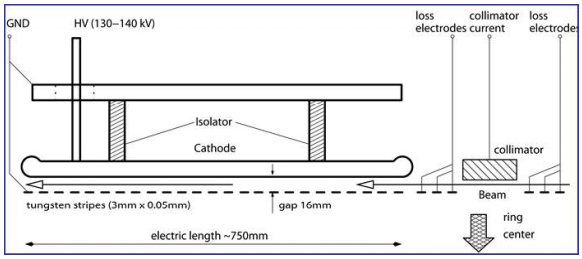

Figure 3. Principle of the electrostatic extraction channel EEC.

radial separation. In this way the gap between the last two turns can be raised from 6 to 18 mm at the PSI ring cyclotron.

A drawing of the ring cyclotron with the electrostatic injection and extraction elements is shown in Fig. 2. The extraction line consists of the electrostatic extraction channel (EEC) followed by the two sector magnets SM1 and SM2 (with the focusing element FM in between) and the magnetic transport line composed of the magnetic septum AHA and the AHB bend. The electrostatic element EEC is composed of a series of 50 μm thick tungsten stripes set to ground potential and placed in-between the last two turns of the ring cyclotron (Fig. 3). Thanks to this very thin structure, beam losses due to scattering are minimized. The cathode is located outside of the last turn and operates at a potential of -145 kV. The high voltage gap is 16 mm broad with an effective length of 920 mm. The total deflecting angle is $\theta_{beam} = 8.2$ mrad.

3. Beam transport to the SINQ target

After being extracted from the ring cyclotron, the beam is guided to the meson production targets M and E and eventually to the SINQ spallation source. Figure 4 represents the horizontal (x) and vertical (y) beam envelopes over the 116 m long transport channel. Light blue elements represent bending magnets while the red ones are quandrupoles. Collimator apertures are depicted as black arrows. Green areas represent the target regions where significant amounts of beam are lost. Away from targets, the average loss rate is as low as 1 nA/m (0.6 W/m). Figure 4 was obtained by putting together beam envelope fits of the three beam line sections ring extraction to target M, target M to target E and from target E to SINQ. Such fits are routinely performed at PSI employing the beam profiles measured by over fifty horizontal and vertical beam profile monitors and fitting the 2σ beam widths by means of the TRANSPORT computer code [5]. At the location of the meson production targets M and E, the 2σ beam widths are of the order of 1.5 mm and 2.5 mm in the horizontal and vertical plane respectively. Considering a Gaussian beam distribution, this translates into a peak beam power density of almost 200 kW/mm^2. Target M absorbs about 1% of the beam without a significant change

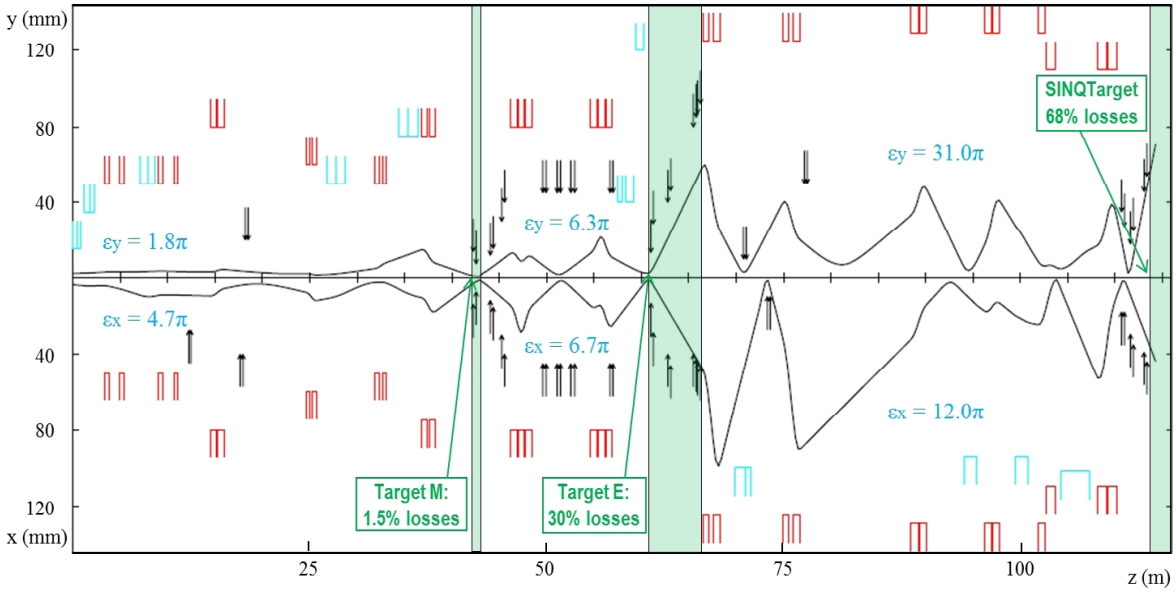

Figure 4. Horizontal and vertical beam envelopes along the PSI high intensity transport line starting from the ring extraction. Beam emittances (2σ) are expressed in unit of mm·mrad and refer to the non-dispersive component.

of the beam energy. The target is composed of a 5 mm thick graphite wheel rotating at a frequency of 1 Hz and shielded against beam misalignment by a Densimet® collimator. The beam transport between target M and target E in handled through a dispersion free beam line section composed of two quadrupole triplets. Two copper collimators are installed 1 m and 2 m downstream of target M respectively in order to shield the beam line components from large angle scattered protons. Between the two triplets and inside the last quadrupole, the vacuum pipe is furnished with four built-in 316L-steel collimators, each of them protecting a beam profile monitor from uncontrolled beam loss. Up to target E, the proton beam transport line is equipped with over 30 beam position monitors (BPMs). These diagnostic devices are integrated in an automatic beam position control system making use of the BPMs signals in order to control a similar number of steering magnets. Furthermore, the beam position and tilt in front of target E can be adjusted by means of a bump formed by three bending magnets. The design of the meson production target E is similar to the one of target M, but the thickness of the rotating wheel is 8 times larger (40 mm). This causes beam energy degradation from 590 to 575 MeV. Beam absorption and losses are also significant. Around 8% of the beam is absorbed by the target material, while about 21% is cut away by a group of four oxigen free copper (OHFC) collimators (Fig. 5) or lost in the local shielding. This collimation system, installed between target E and the first magnetic element, can be subdivided into two subsystems: the first two collimators (C0-C1) shield the beam line from large angle scattered beam particles, while the second pair (C2-C3) reshapes the proton beam leaving the target E region in order to match the geometric acceptance of the SINQ beam line. A pair of vertical and horizontal movable slits located 5 and 7 m downstream of C3 respectively capture halo particles originating from scattering off C2-C3. The C2-C3 water cooled collimator system is located 4.7 m downstream of target E. Each collimator is 30 cm long, has an elliptical cross section and a segmented structure made of teeth whose thickness grows along the radial as well as the longitudinal direction. In the present configuration, the collimators' elliptical aperture diverges along the beam direction in order to follow the increasing beam envelope. The collimator system was originally designed to withstand

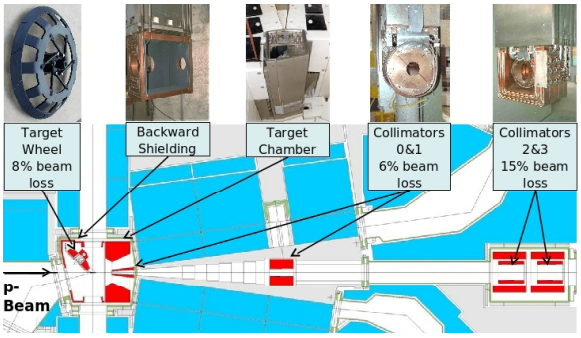

Figure 5. Horizontal cut through the target E region at the proton beam plane.

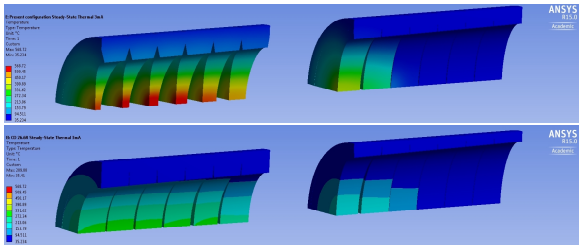

Figure 6. ANSYS simulation of the temperature distribution (same scale) in the collimators C2 (left) and C3 for the current (top) and the proposed new design (bottom).

2 mA (1.2 MW) beam current. ANSYS [4] simulations showed that, at 3.0 mA, C2 would reach a peak temperature of 570 °C in case of an aligned beam (Fig. 6). This value is well beyond the accepted safety limit of 405°C, corresponding to 50% of the melting temperature of copper. For this reason, a simulation based optimization of the collimator design was started [5, 6] and accomplished in 2014 [5, 7]. Turtle [8] beam line simulations have shown that a 12.5% widening of the collimator system aperture would be compatible with the beam line acceptance and would not have any negative impact on the loss rate on the beam line components located downstream of C3. Moreover, the shielded region located directly downstream of the collimators would profit from the decreased scattering rate and the overall beam line transmission would raise by about 4%. A slight re-tuning of the beam optics would allow to keep the beam footprint at the SINQ target window almost unaltered. This outcome represents the starting point for the optimization of the collimator geometry performed by means of ANSYS. The proposed new design exhibits a 12.5% wider opening at the downstream end of C3, thicker teeth (C2) and a convergent-divergent (C2-C3) aperture scheme. The results are a much more uniform temperature distribution and a peak temperature at 3.0 mA of only 290 °C in case of aligned beam (Fig. 6) and 386 °C considering a 1 mrad beam tilt.
Up to target E the bending plane is horizontal. However, SINQ has a vertical bending plane. After leaving the target E region, the beam reaches the dipole magnet AHL that deflects the protons downwards, 11 m below the level of target E. Three other bends then turn the beam upwards in order to reach the SINQ target from below. The last quadrupole doublet defocuses the beam such that at the target entrance the beam footprint presents an elliptical cross section with $2\sigma_x = 44$ mm and $2\sigma_y = 58$ mm. Three copper collimators installed immediately before the end of the beam line shield the rim of the target entrance window and, at the same time, prevent activation of the beam line components from back scattered neutrons. A review of the SINQ target can be found in [9].

4. The UCN beam line

Since August 2011, the UCN spallation source is operated at the PSI-HIPA complex. The concurrent operation of UCN and SINQ is made possible by a pulsing system that switches the entire 1.4 MW beam between the SINQ and UCN beam lines with a duty cycle of 1%. The typical pulse length is 6 s, with a maximum allowed duration of 8 s. During the UCN pulse, neutrons arising from the target are first thermalized in liquid D_2O and then cooled down to UCN in a deuterium crystal kept at 5 K. The generated ultra-cold neutrons are stored in a tank and eventually guided to the experiments. A drawing of the UCN beam line is presented in Fig. 7. The heart of the beam switching system is a small, air-cooled, fast kicker magnet installed about 12 m downstream of the ring extraction point. The 6 mrad tilt given by the kicker produces

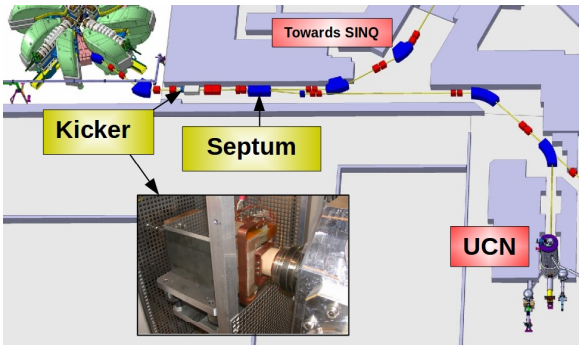

Figure 7. Drawing of the UCN beam line along with a picture of the kicker magnet.

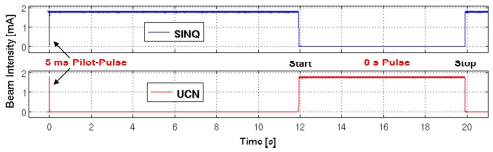

Figure 8. The first 8 s long megawatt UCN beam pulse produced in December 2011.

a 40 mm horizontal displacement seven meters downstream, thus allowing the beam to enter a magnetic septum getting diverted into the UCN beam line. During the transition, the beam is absorbed by a tungsten collimator installed at the upstream end of the septum. In order to limit activation, the switchover time has to be kept as short as possible. For this reason, the timing of the kicker power supply has been tuned such that the first 85% of the beam angular deflection is reached within 1 ms. Under these conditions, considering a UCN operation of one pulse every 200 s without interruptions over one year, calculations have shown that, after 15 days decay time, the collimator dose rate does not exceed 65 mSv/h at a distance of 3 cm from its surface. Nevertheless, instantaneous losses on the collimator are too large for the machine protection system. Hence, in order to prevent beam trips, the interlock thresholds of several beam loss monitors are substantially raised during 3 ms at the beginning of each kick. The actual UCN transport line begins at the location of the septum and guides the beam over 46 m towards the UCN source. Ten meters upstream of the target, the beam is blown up by a quadrupole magnet and then collimated so that at the target entrance it gets a circular footprint with a 4σ diameter of 160 mm. The kicking scheme includes at least one 7 ms short pilot pulse before each several seconds long UCN production pulse. This procedure was implemented in order to check that the proton beam is well centered already at the start of the production pulse. During the pilot pulse, the beam position is measured by 14 BPMs and 4 harp monitors. If the beam displacement exceeds the tolerance level, a centering step is performed and a new pilot pulse is kicked into the UCN beam line. The commissioning of the UCN started in 2008 and lasted three years. During this time the UCN source was not yet ready, therefore the beam line was developed and tested by employing a small beam dump installed for this purpose downstream of the last bending magnet. In December 2010, the first 8 s long megawatt beam pulse was produced (Fig. 8).

5. Simulation of a beam flattening system for SINQ

The spallation region of the SINQ target is composed of a rod bundle with over 30 rows of zircaloy tubes filled with lead, actively cooled by D_2O. The highly inhomogeneous Gaussian proton beam causes thermomechanical stresses that could lead, on the long term, to damage the target structure. This is a critical issue for the beam current upgrade program. In the SINQ beam line, the employment of non-linear magnetic elements, like octupoles, to fold beam fringes is ruled out because of the strong influence of such elements on the footprint shape. Additionally, octupole fields generate sharply peaked beam edges that would cause large activation of the three SINQ collimators. On top of that, due to lack of space, these elements could not be installed without a major reshuffle of the proton beam line. A relatively simple way of flattening the

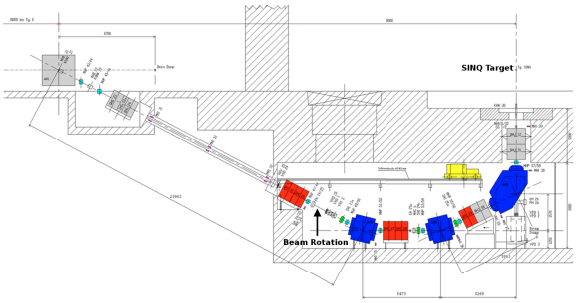

Figure 9. Layout of the SINQ beam line with the possible location of a beam rotation system, indicated by an arrow.

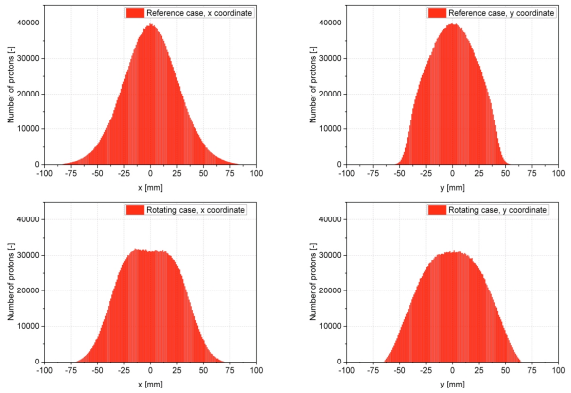

Figure 10. Turtle simulation of proton beam transverse distributions at the SINQ target entrance window with present optics (top) and applying a beam rotation system (bottom).

beam distribution could be accomplished by means of a beam rotation system [10]. The space needed for the installation of the two small dipoles would be available some 24 m upstream of the SINQ target entrance window (Fig. 9). Beam optics simulations were carried out with the goal of getting an efficient beam flattening with reasonable losses at the SINQ collimators. The resulting beam distribution (shown in Fig. 10 along with the present one) exhibits a 50% reduction of the peak current density (from 36.5 to 17.7 μA/cm^2). The energy deposition in the SINQ target and the effect of the beam rotation on the neutron flux were simulated with the Monte Carlo code MCNPX [11]. In order to start with a realistic source, the proton beam distributions generated by means of Turtle were used as input for MCNPX. The comparison of the peak energy deposition in the central rods over the target length for the present and the rotating beam (Fig. 11) shows the benefits of the beam rotation. Furthermore, a significant decline in the neutron production was ruled out. Nevertheless, due to the rotation of the proton beam, a time dependent oscillation of the neutron fluxes from the cold source has to be expected.

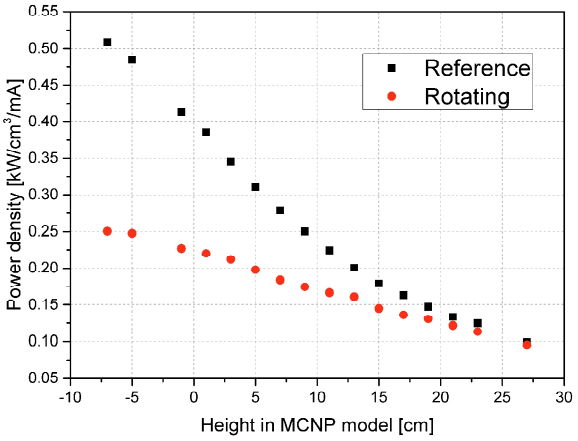

Figure 11. Peak energy deposition in the central rods along the target.

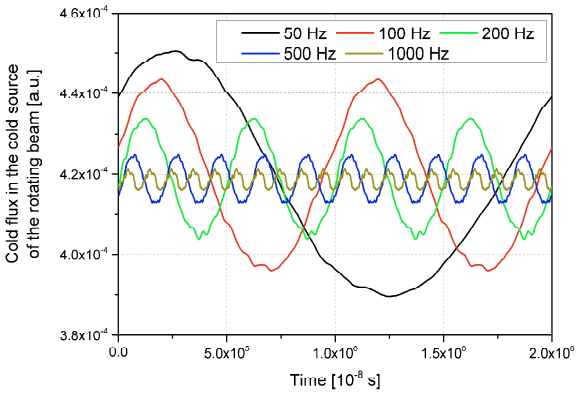

Figure 12. The time-dependent cold neutron flux in the cold D_2 source with different rotation frequencies.

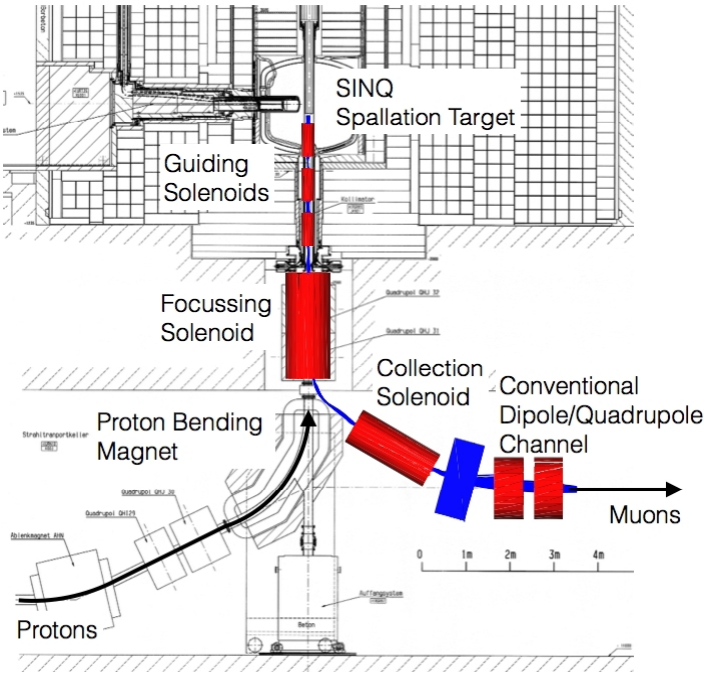

Figure 13. Schematics of the SINQ surface muons extraction concept. 28 MeV/c momentum backscattered muons are guided and focusses along the proton beam line by means of solenoid magnets before being deflected into a dedicated beam line through the fringing field of the last dipole magnet of the proton beam.

This modulation was simulated for different rotation frequencies (Fig. 12). In order to limit the cold neutron flux modulation to less than 2%, a rotation frequency on the order of 1000 Hz is required.

6. Study of surface muons extraction from SINQ

High rate muon beams are highly demanded tools both in applied and fundamental research. Solid state physicists exploit the so-called muon spin resonance (μSR) technique in order to probe the microscopic properties of novel materials. In particle physics, the search for lepton number violating processes, measurements of the muon decay properties as well as studies of muonic atoms decay are carried out by means of precision experiments relying on the availability of intense muon beams. At the PSI-HIPA facility muon rates of up to $4 \cdot 10^8$ μ/s are currently available at the target E secondary beam lines. Simulations have shown that this already remarkable figure could be substantially increased if one could collect the muons coming from the decay of pions produced in the neutron spallation target of the SINQ facility and stopped in its beam entrance window. A schematic showing the working principle of this concept is given in Fig. 13. Potentially, muon rates on the order of 10^{10} μ/s could be achieved in this way. The feasibility of this project is being assessed by a two year study currently carried out at PSI. Results are expected by mid 2015.

7. Conclusion

The PSI-HIPA 1.4 MW proton machine is a very well established facility and, after four decades, still at the forefront of the intensity frontier. Room for a stepwise improvement up to 1.8 MW is available and requires optimization of crucial aspects like extraction losses, beam collimation after target E as well as beam energy deposition on the SINQ target. An improved design of the target E collimator system was recently proposed and the manufacturing should be carried out within the next two years. The preliminary design of a beam rotation system for the SINQ spallation source at PSI was presented. Results showed that the beam rotation would bring substantial benefits in terms of distribution of the energy deposition in the SINQ target without affecting the neutron spectrum and yield. In order to limit the amplitude modulation of the

neutron flux, a rotation frequency in the order of 1 kHz is required. Another interesting idea currently under investigation is the possibility of exploiting the SINQ target as a high intensity source of surface muons.

References

[1] M. Seidel et al., "Production of a 1.3 MW proton beam at PSI" IPAC10, Kyoto, Japan, May 23-28, 2010.
[2] D. Reggiani et al., "A macro-pulsed 1.2 MW beam for the PSI ultra-cold neutron source", PAC09, Vancouver, Canada, May, 4-9, 2009.
[3] B. Lauss, "Ultracold neutron production at the second spallation target of the Paul Scherrer Institute", Proceedings of the ESS Science Symposium on Neutron Particle Physics at Long Pulse Spallation Sources 2013, Physics Procedia, Volume 51, pp 98101 (2014).
[4] ANSYS, Inc., http://www.ansys.com/
[5] D. Reggiani et al., "Beam Transport Optimization Studies of the PSI MW-Class Proton Channel", IPAC14, Dresden, Germany, June 15-19, 2014.
[6] Y. Lee et al., "New Design of a Collimator System at the PSI Proton Accelerator", HB2010, Morschach, Switzerland, September 27 - October 1, 2010.
[7] R. Sobbia et al., "PSI Technical memorandum", in progress.
[8] U. Rohrer, "Graphic Transport/Turtle Framework", http://aea.web.psi.ch/Urs_Rohrer/MyWeb
[9] W. Wagner, "PSIs experience with high-power target design and operation", 3rd High-Power Target Workshop, Bad Zurzach, Switzerland, September 10-14, 2007.
[10] D. Reggiani et al., "Simulation of a beam rotation system for the SINQ spallation source at PSI" IPAC'13, Shanghai, China, May 12-17, 2013.
[11] D.B. Pelowitz (ed.), "MCNPX User's Manual Version 2.7.0", Los Alamos National Laboratory Report, LA-CP-11-00438, April 2011.